

## Supplementary material

### Trial-by-trial source-resolved EEG responses to gait task challenges predict subsequent step adaptation

Johanna Wagner\*, Ramon Martinez-Cancino, Scott Makeig

**1. The SDN after step-advance perturbations.** Why an SDN equivalent does not clearly appear nor significantly predict adaptation step size during step-advance perturbations is not entirely clear. Negative-going ERP peaks following step-advance shifts were notably smaller compared to step-delay perturbations, and the pMFC source cluster only accounted for 23% of grand-mean ERP variance between 100 ms and 350 ms following  $C_0$  in step-advance shift trials. Single trial step-advance negativities in this time range were also notably more variable over subjects in both latency and amplitude. Here we show a figure illustrating the mean and trial-by-trial response to step-advance tempo shifts.

Figure S1(A) visualizes the envelopes of the component cluster projections that explained, in total, 93.4% of the variance (pvaf) in the summed scalp ERP contributions of the 9 selected IC brain source clusters in the step-advance condition. To visualize the relationships between the ERP complex and step length for step-advance perturbations we plotted single trial ERP-image plots (see Fig. S1B). For these plots, first we time warped single-trial ERPs to the median cue latencies (across subjects) using piecewise linear interpolation. This procedure aligned time points of the two cues following the cue  $C_0$  that signaled the tempo shift (e.g.,  $C_1$  and  $C_2$ ).

Then we sorted single trials for ICs in the pFMC cluster by step length of the first post-shift steps,  $SOA_{0,1}$  (shown here) and  $SOA_{1,2}$  (not shown). After sorting, the images were smoothed over trials with a 30-trial moving average. Step measures were normalized in proportion to the baseline cue tempo. The ERP-image plot below (B) shows that a larger negative deflection in the source resolved EEG predicts a smaller step response  $SOA_{0,1}$ . Note the relatively smaller and slightly earlier negativity  $\sim 200$  ms after onsets of  $C_0$  tones representing step-advance shifts -- near-only in trials in which the shift cue occurred *before* the heel strike  $S_0$  (e.g., trials  $\sim 350$  to 500 below).

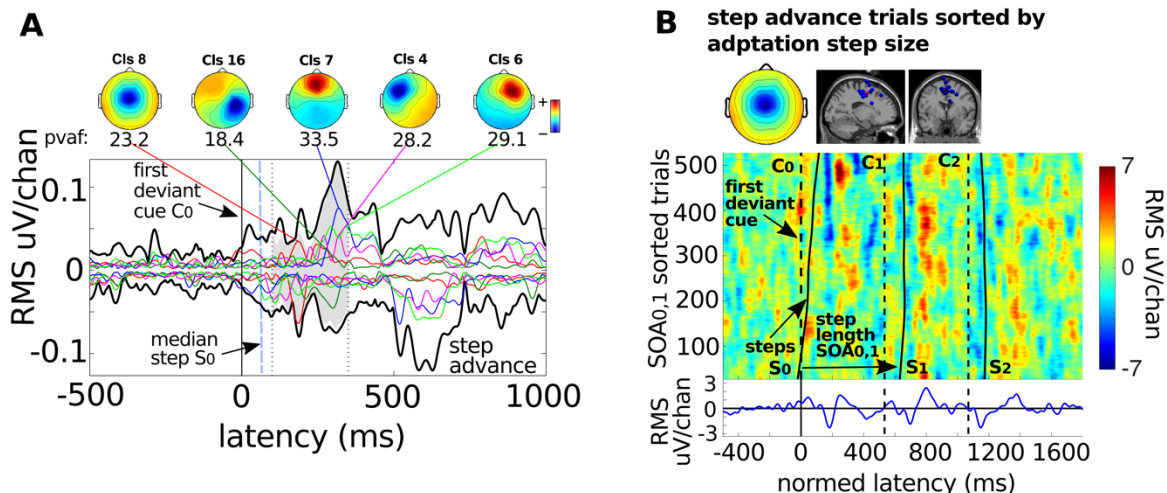


**Figure S1. Source cluster contributions to ERPs time locked to the first latency-perturbed cue presentation and single-trial ERPs sorted by adaptation step length for step-advance trials:** **A.** (colored traces) ERP envelopes for the 5 largest-contributing (in the 100-350 ms time range between the dotted lines) source clusters (cluster-mean scalp maps shown) versus the ‘sum of all 9 clusters’ ERP envelope (black traces). **B.** Top panel: cluster mean scalp map and equivalent current dipoles for the pFMC cluster. Center panel: Single-trial ERPs were pooled across cluster ICs and sorted by  $SOA_{0,1}$ . Blue indicates a negative deflection, red indicates a positive deflection. Dashed black vertical lines represent cues, continuous black vertical lines represent steps. The figure shows that trials with larger negative deflections around 200-300 ms predict a smaller step response in the unfolding step interval ( $SOA_{0,1}$ ). Bottom panel: Grand mean cluster ERP.

This relationship was only present for  $SOA_{0,1}$  but not for  $SOA_{1,2}$ . Sorting order of step size is reversed here compared to step delay ERP-image plots meaning that smaller steps are displayed at the top while larger steps are displayed at the bottom of the ERP-image.

**2. Time warping and smoothing of ERP-image plots.** For illustration we plotted non-time warped ERP images with smoothing over a trial average of 30 trials (Fig. S2A) and over 3 trials (Fig. S2B). Single-trial ERPs time locked to  $C_0$  were pooled across pMFC-cluster ICs and sorted by length of the adaptation step  $SOA_{1,2}$ . After sorting, the images were smoothed over adjacent trials with a 30-trial moving average (panel A) or over a 3-trial moving average (panel B). As you can see the relationship between the SDN and  $SOA_{1,2}$  remains preserved without time warping and is visible with a lower number of trial averages. Upper trials, in which the participant made a larger  $SOA_{1,2}$  adaptation step, exhibit a stronger SDN near 250 ms.

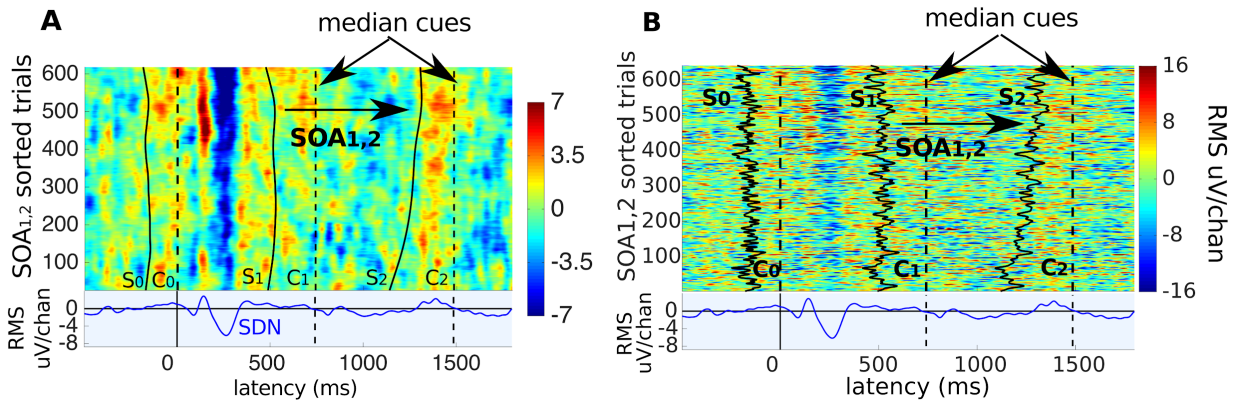


**Figure S2. Single-trial ERPs sorted by adaptation step size.** Single-trial ERPs time locked to  $C_0$  were pooled across pMFC-cluster ICs and sorted by adaptation step size ( $SOA_{1,2}$ ). After sorting, the images were smoothed over adjacent trials with a 30-trial moving average (panel A) or over a 3-trial moving average (panel B). Blue indicates negative activation; red, positive activation (green: 0). Dashed black vertical lines represent cue onsets; solid black traces represent heel strikes of adaptation steps  $S_0$  through  $S_2$ . Upper trials in which the participant made a larger  $SOA_{1,2}$  adaptation step exhibit a stronger SDN near 250 ms. Bottom panel: The cluster-mean ERP.

**3. Details of the pMFC cluster.** Below we show details of the pMFC cluster: the IC scalp maps, power spectra and Event-related Spectral Perturbations (ERSPs, Makeig, 1993) time locked to  $S_0$ .

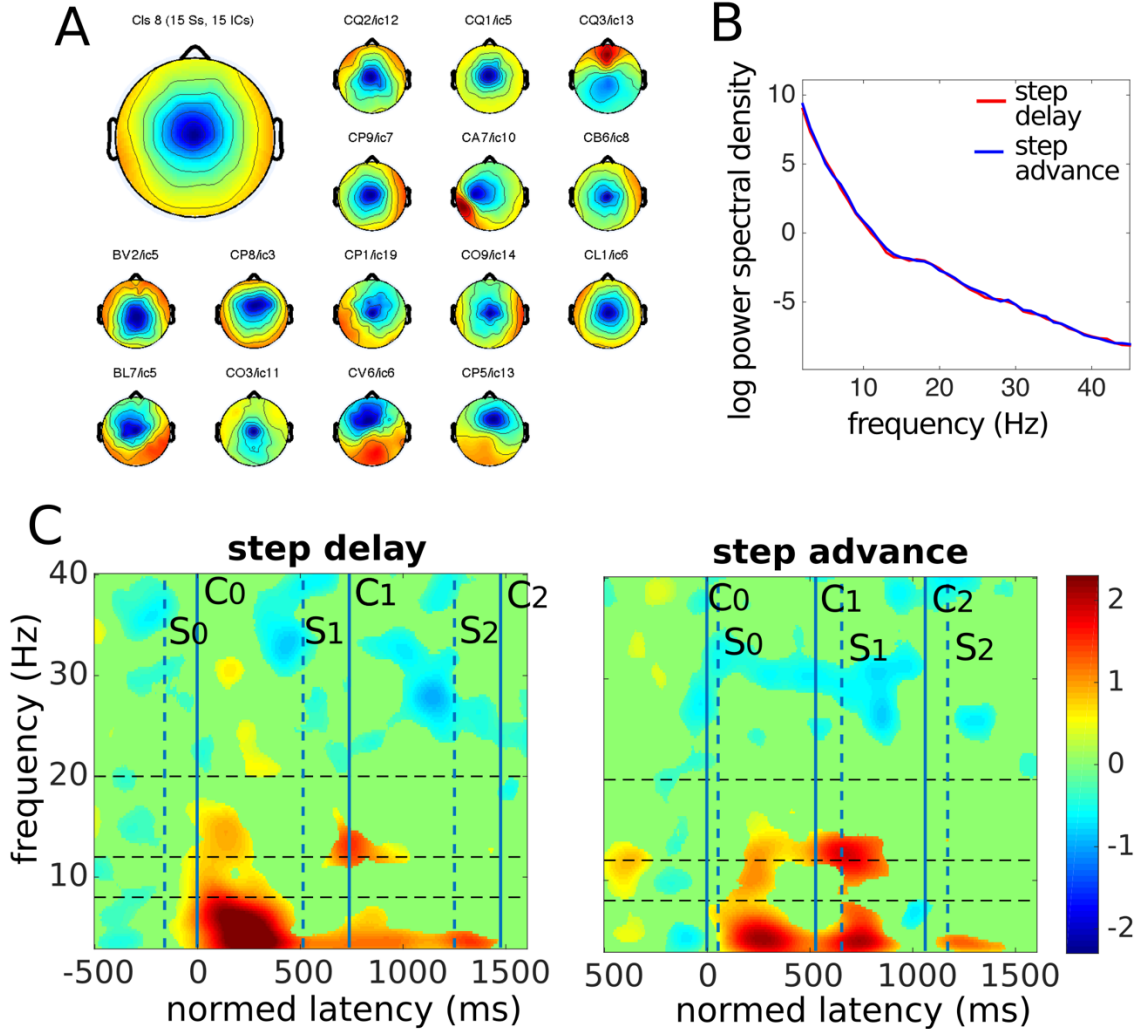


**Figure S3.** Single scalp maps of ICs comprising the pMFC cluster (A), cluster average spectrum (B) and cluster average ERSP for step advance and step delay perturbations (C) ERSP images time locked to step-delay (left) and step-advance (right) perturbations. ERSPs are locked to  $C_0$  and timewarped to  $C_1$  and  $C_2$ . Single-trial log spectrograms were time warped to median cue latencies of  $C_1$  and  $C_2$  before averaging. Log mean power at each frequency in the interval  $-1$  s to  $0$  s preceding the tempo shift was subtracted from the log spectrum at each latency to obtain relative changes in log spectral power. Nonsignificant changes from baseline are masked in green.

ERSPs were computed for each IC. For ERSPs we segmented the data from  $-1$  s to  $3$  s around  $C_0$ . Single-trial spectrograms were computed and linearly time warped to median cue

latencies (across subjects) using linear interpolation as implemented in the eeglab function *newtimef()*. This procedure aligned the latencies of  $C_1$  and  $C_2$  over trials following each tempo shift to their median values. Relative changes in spectral power were obtained by computing the mean difference between each single-trial log spectrogram and the mean baseline spectrum (the average log spectrum between  $-1$  s and  $0$  s preceding tempo shifts). Significant deviations from the baseline were detected using a nonparametric bootstrap approach (Delorme and Makeig, 2004) and corrected for multiple comparisons using false discovery rate (Benjamini and Yekutieli, 2001).

Both step-advance and step-delay perturbations show a typical power increase in theta band power, as has been shown in prior literature on error-related potentials (Luu et al., 2004). ERSP maps of the pMFC cluster do not exhibit a broadband power increase which could be indicative of movement artifact (see Fig. S4 below and Castermans et al., 2014; Kline et al., 2015).

**4. Artifacts during walking.** To examine the morphology of the SDN relative to movement and muscle artefacts, we clustered artifact ICs and plotted scalp maps, time-courses, spectra, and ERSPs for a movement artifact cluster. The time course of this cluster ( $-0.5$  s to  $+2$  s around  $C_0$ ) clearly shows the movement artifacts occurring rhythmically time locked to the ongoing step cycle. Figure S4B shows clearly that movement artifacts have a different morphology compared to the SDN we observed in pMFC. Movement artifact time courses peak shortly after each step,  $S_0$  and later steps  $S_1$ ,  $S_2$ , etc.. ERSPs (Fig. S4C) of movement artefacts show typical broad band modulations over frequency bands as shown before in Castermans et al., (2014) and Kline et al., (2015).

It is important to mention that all ICs contained in the movement artefact cluster had equivalent dipoles that explained less than 70% of their scalp projection. This result is in line with Snyder et al., (2015) who recorded pure movement artefact data during walking with a swim cap as a non-conductive layer underneath the EEG cap. Snyder et al., 2015 showed that source separation with ICA and subsequent single equivalent current dipole localization located 99% of the obtained pure artifact sources outside the head or lacking dipolar characteristics (less than 85% explained variance).

Figure 5S displays average and single IC time courses relative to  $C_0$  and shows that single movement artefact ICs have similar time courses as the movement artefact cluster average time course. Figure S4B and Figure S5 clearly show that the time course of the movement artefact cluster is different from the SDN. We also plotted scalp map, time-course and spectra for two clusters related to EMG activity (see Fig. S6 below). The spectra show typical low power at lower frequencies and an increase in power over 20Hz. This is clearly different from the  $1/f$  spectrum inherent to EEG activity. Again the time course plotted relative to  $C_0$  in both EMG clusters look nothing like the SDN we found in the pMFC cluster.

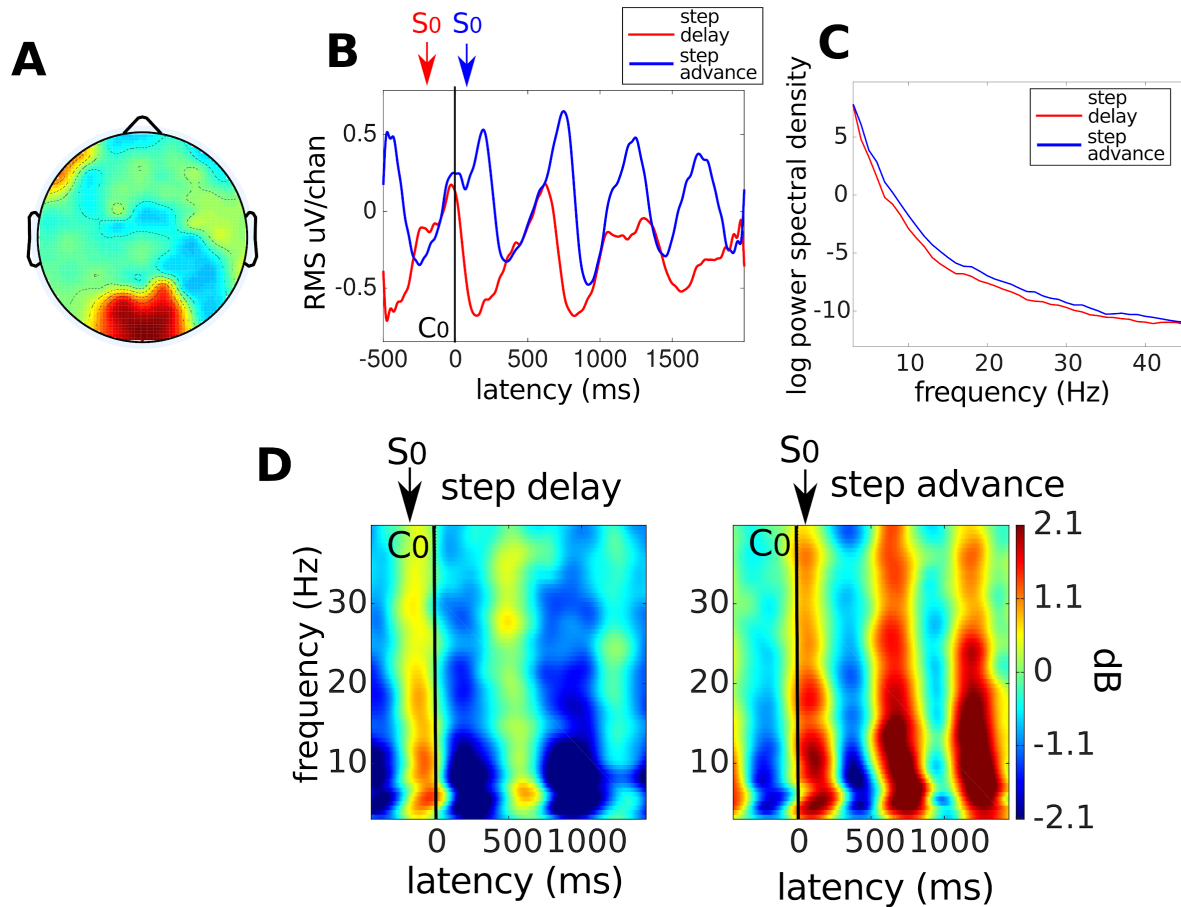


**Figure S4:** (A) Average scalp map of ICs comprising a cluster related to movement artifacts; (B) cluster-mean time courses relative to  $C_0$ . Movement artifact time courses peak shortly after each step and clearly have a different morphology from the SDN. (C) cluster-mean log spectra for step-advance and step-delay perturbations, time locked to  $C_0$ . (D). Movement artifact ERSPs show the same broadband power modulations as has been shown previously for these types of artifacts (Castermans et al., 2014, Kline et al., 2015). ERSPs here are not corrected for significance.

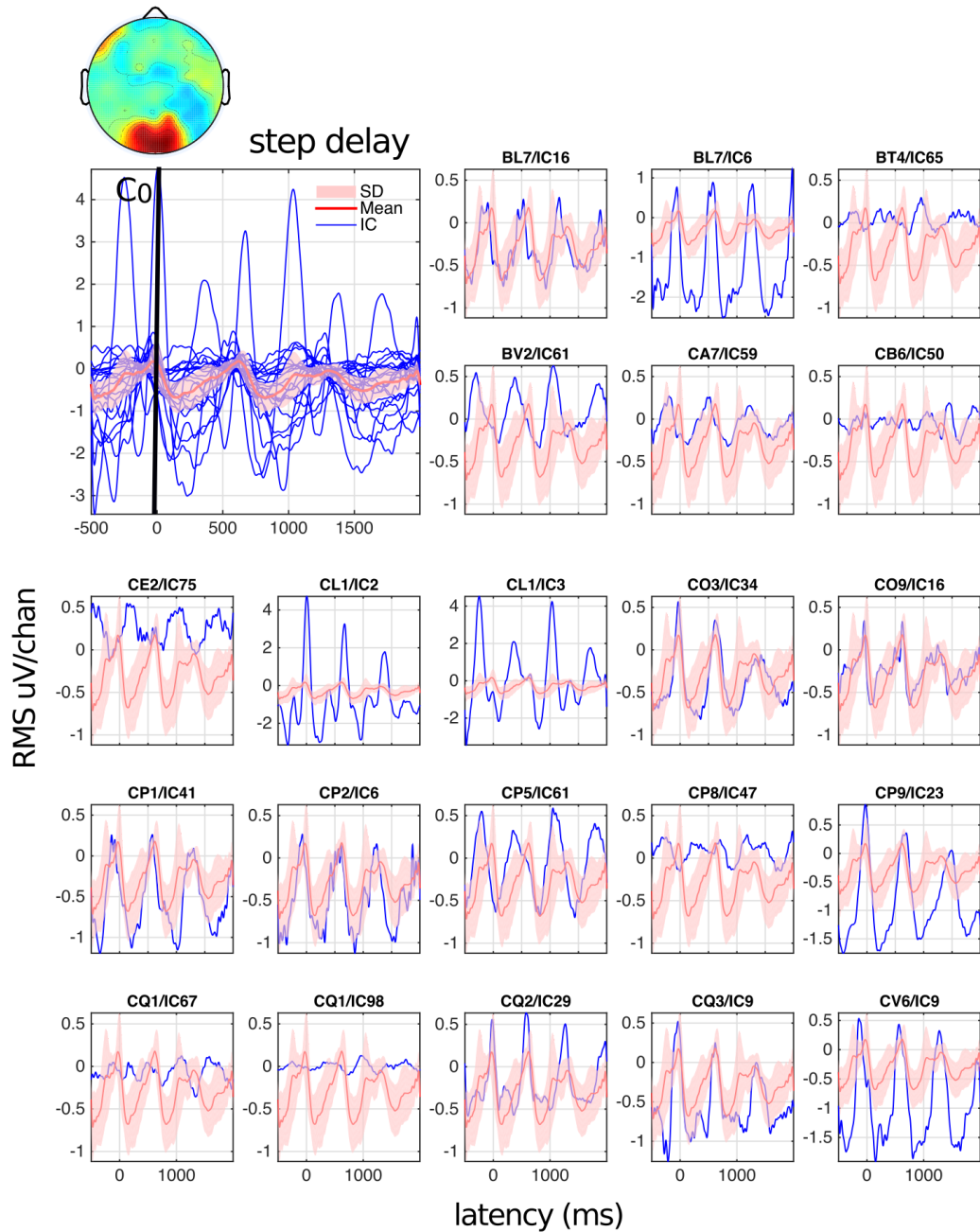


**Figure S5:** Cluster-mean and single-IC time courses relative to  $C_0$  for ICs comprising a cluster related to movement artefacts. Blue trace- represent single IC time courses, red lines represent the cluster-mean time course relative to  $C_0$ , the pink shaded background represents one standard deviation of the average time course. As shown in Figure S4B, the movement artefacts peak short after each step and have a clearly different morphology from the SDN.

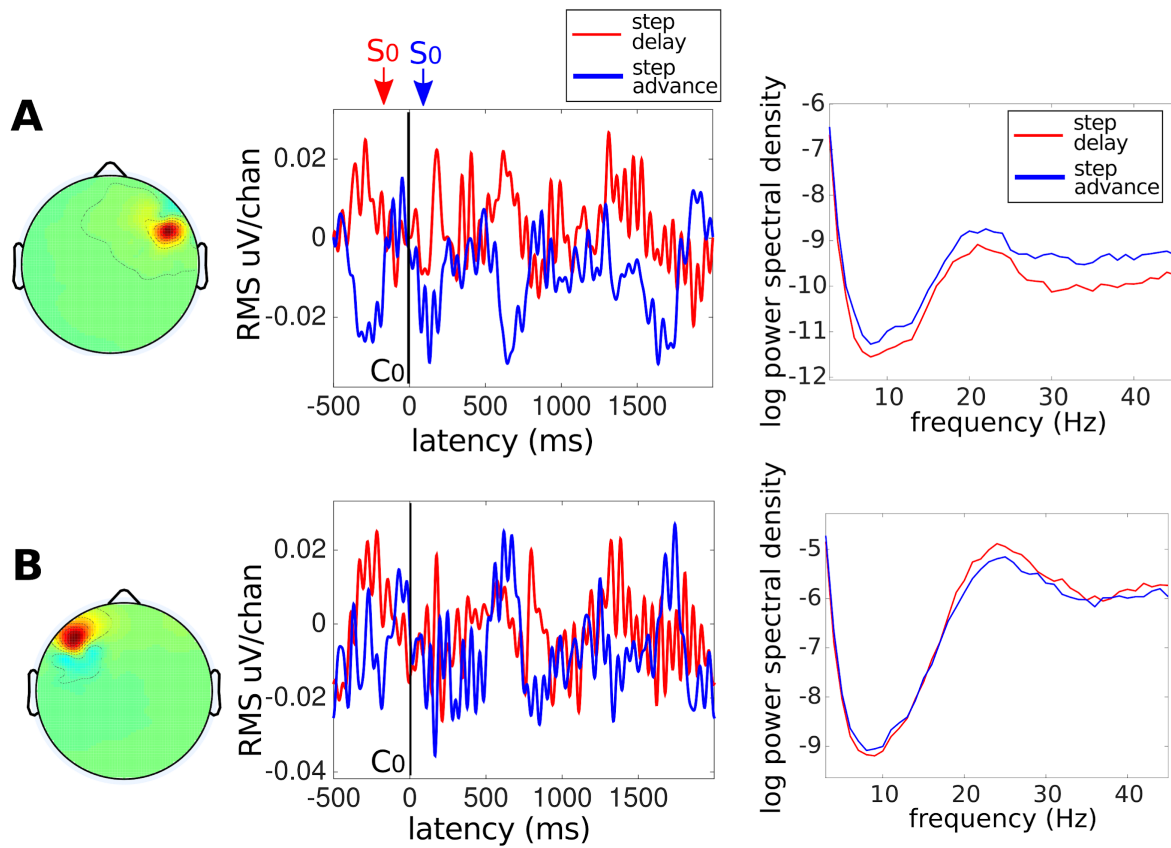


**Figure S6:** Average scalp map of ICs comprising two clusters related to scalp EMG on the right (A) and on the left (B) side of the scalp. In each row from left to right: Cluster-mean scalp map, cluster-mean time courses relative to  $C_0$  and cluster-mean spectra. The spectra of both clusters show a typical power distribution for EMG activity: Low power at lower frequency and increase in power at frequencies above 20 Hz.